BIOCHEMICAL PHARMACOLOGY 73 (2007) 1715–1726

available at www.sciencedirect.com

ScienceDirect

journal homepage: www.elsevier.com/locate/biochempharm

Inhibition of G1/S transition potentiates oxaliplatin-induced cell death in colon cancer cell lines

Tatiana V. Rakitina [1,2], *Irina A. Vasilevskaya* [1,*], *Peter J. O'Dwyer*

Abramson Family Cancer Center, University of Pennsylvania, 1020 BRB II/III, 421 Curie Blvd, Philadelphia, PA 19104, USA

ARTICLE INFO

Article history:
Received 1 December 2006
Accepted 31 January 2007

Keywords:
Oxaliplatin
17-AAG
Cell death
p21
Cell cycle
Cdk modulators

ABSTRACT

In a series of colorectal cancer cell lines, both necrosis and apoptosis were induced upon exposure to oxaliplatin, and enhanced by co-administration of the Hsp90 inhibitor 17-AAG. We analyzed the effects of these interventions on the cell cycle, and found that oxaliplatin treatment caused G1 and G2 arrest in HCT116 cells, and S-phase accumulation in two p53-deficient cell lines (HT29 and DLD1). Addition of 17-AAG enhanced cell cycle effects of oxaliplatin in HCT116, and induced G1 arrest and decrease in S-phase population in the other cell lines. Analysis of cell cycle proteins revealed that the major difference between the cell lines was that in HCT116, 17-AAG resulted in profound inhibition of expression and phosphorylation of late G1 proteins cyclin E and cdk2, with no effect on p21/WAF1 induction. Consistent with these, an HCT116 $p53^{-/-}$ line, lacking p21, showed resistance to oxaliplatin, failure to enter apoptosis, and an accumulation of cells in S-phase. Introduction of p21 in these cells caused reversal of that phenotype, including restoration of the G1 block and re-sensitization to oxaliplatin. Inhibition of G1/S progression using cdk2 inhibitor also enhanced oxaliplatin cytotoxicity. We conclude that in colon cancer cells with impaired p53 function, interventions directed to cycle arrest in G1 may potentiate oxaliplatin activity.

1. Introduction

Oxaliplatin (DACH-(oxalate)platinum II, L-OHP), a third generation platinum compound with therapeutic activity in colorectal cancer, was developed based on the structure of its diaminocyclohexane carrier group which confers a pattern of tumor specificity different from that of cisplatin [1]. In colon cancer, oxaliplatin is established as the optimal initial treatment for metastatic disease, and has recently been shown to benefit patients receiving adjuvant post-surgical chemotherapy [2]. As with cisplatin, oxaliplatin resistance has been associated with accumulation of detoxication enzymes and transporters [3–5], as well as nucleotide excision repair enzymes [5–7]. Its cytotoxicity appears to depend also on modulation of apoptotic pathways by pro- and antiapoptotic Bcl-2 family members including Bax, Bak, and Bcl-xL [8–10], and by Fas [11]. A number of genes with known roles in apoptosis were identified by cDNA microarray as possible predictors of the response to oxaliplatin, but the role of tumor suppressor p53 is unclear [9].

We previously demonstrated that the Hsp90 inhibitor, 17-AAG (17-allylamino-17-demethoxy-geldanamycin) [12], promotes oxaliplatin-dependent caspase activation and cytotoxicity by down-regulation of antiapoptotic signaling through the

* *Corresponding author*. Tel.: +1 215 573 7300; fax: +1 215 573 7049.
E-mail address: vasilevs@mail.med.upenn.edu (I.A. Vasilevskaya).

[1] These authors have contributed equally to this work.

[2] Present address: Shemyakin-Ovchinnikov Institute of Bioorganic Chemistry, Russian Academy of Sciences, Moscow, Russia.

0006-2952/$ – see front matter © 2007 Published by Elsevier Inc.
doi:10.1016/j.bcp.2007.01.037

transcription factor NF-κB [13]. In a panel of four colon cancer cell lines with differing p53 status the effect of the combination varied with the type of cytotoxicity assay used: MTT and colony-forming assays revealed additivity or synergy in p53-positive HCT116 and antagonism or additivity in p53-deficient HT29, respectively, with two other p53-deficient cell lines in intermediate positions. These data suggested that both oxaliplatin and 17-AAG contribute to the antiproliferative effects of the combination. Another study of oxaliplatin and irinotecan in combination in HT29 colon cancer cells [14] revealed that oxaliplatin can inhibit cell proliferation without inducing cell death, and may cause cell death by necrosis more commonly than by apoptosis. We wished to further understand the relationship between oxaliplatin-induced cell death and its cell cycle effects in human colon cancer cells, and explored this using 17-AAG, a strong inducer of G1 arrest.

We found that functional p53 was associated with greater susceptibility of cells to oxaliplatin-induced apoptosis. Necrosis was the prevailing mechanism of cell death in p53-deficient cells. 17-AAG could facilitate both apoptotic and necrotic cell death with oxaliplatin, but the combination was more effective in cells with functional p53. The basis of this difference was determined in part by cell cycle responses to oxaliplatin: in p53-deficient cells S-phase delay was associated with resistance. In these cells 17-AAG has potentiated G1 arrest through an effect on G1 cyclin/cdk (cyclin-dependent kinase) complexes. HCT116/p53$^{-/-}$ cells, lacking p53 and, consequently, p21 functions, displayed a resistant profile with a similar S-phase delay; restoration of p21 by transfection, or its mimicking by pharmacologic cdk inhibition, sensitized cells to oxaliplatin. These data suggest a therapeutic role for cell cycle modulators in combination with oxaliplatin in colon tumors.

2. Materials and methods

2.1. Cell lines and reagents

The colon cancer cell lines HCT116 (wild type p53), and HT29 and DLD1 (non-functional p53), were purchased from American Type Culture Collection (Manassas, VA). The HCT116 p53$^{-/-}$ cell line was a gift from Dr. Bert Vogelstein (John Hopkins Oncology Center, Baltimore, MD). Cells were cultivated in Eagle's MEM supplemented with 10 or 5% (for LDH assay) fetal bovine serum, penicillin, streptomycin (100 units/ml), and fungizone (Invitrogen, Carlsbad, CA). Cultures were maintained in humidified incubator at 37 °C in 5% CO_2–95% air. Oxaliplatin was purchased from LKT Laboratories (St. Paul, MI), dissolved in sterile PBS, aliquoted and stored at −20 °C. 17-AAG was kindly provided by Dr. Edward Sausville (Developmental Therapeutics Program, NCI, Bethesda, MD), dissolved in DMSO, aliquoted and stored at −20 °C. The specific cdk2 inhibitor Compound II (referenced in text as cdk2I) was purchased from Calbiochem (EMD Biosciences, Inc., La Jolla, CA).

The pcDNA3 plasmid was from Invitrogen, and the p21-expressing pcDNA3 construct [15] was kindly provided by Dr. M. Olson (University of Pennsylvania, Philadelphia).

2.2. Transient and stable transfections

HCT116 p53$^{-/-}$ cells were plated into 100 mm dishes (1×10^6 cells/dish) and 20 h later transfected using FuGENE 6 transfection reagent (Roche Applied Science, Indianapolis, IN) with 20 μg of pcDNA3 (Invitrogen) or with pcDNA3-p21 plasmids. Efficiency of transfection (typically 70–85%) was controlled in parallel transfection experiment with pcDNA3-eGFP construct. Twenty hours after transfection, cells were replated for MTT assay, LDH assays, TUNEL assay or cell cycle analysis. The level of expression of p53 and p21 was monitored by Western blot analysis during all harvests. DLD1-derived clones stably expressing either pcDNA3 (DLDpc3) or p21 (DP3) were selected after cultivation in the media containing 0.75 mg/ml of G418 and isolation of individual neo-resistant colonies.

2.3. Drug treatments

Oxaliplatin and 17-AAG were added simultaneously and in equitoxic concentrations proportional to the IC_{50} values derived from MTT assays for each cell line. Unless noted otherwise, drugs were used at concentrations equivalent to 15× IC_{50} for oxaliplatin and 10× IC_{50} for 17-AAG: oxaliplatin, HCT116 and HT29, 10 μM; DLD1, 30 μM; 17-AAG, HT29, 100 nM; HCT116 and DLD1, 500 nM. Cells transfected with the p21 construct were exposed to the same concentrations of oxaliplatin as those of parental lines. Simultaneous administration was chosen to facilitate detection of the molecular interactions in the cellular responses to each drug.

2.4. MTT assay and isobologram analysis

The cytotoxicity of oxaliplatin against HCT116 p53$^{-/-}$ transfected with pcDNA3 (HCTp53-/vect) or with pcDNA3-p21 (HCTp53-/p21) was determined by the MTT (3-(4,5-dimethylthiazol-2-yl)-2,5-diphenyltetrazolium bromide) assay: 20 h after transfection cells were plated in 96-well plates at a density of 2000 cells per well; 20 h later oxaliplatin was added for 72 h in concentrations of 0, 0.3, 0.6, 1.2, 2.4 and 4.8 μM. The results of MTT assays were quantified using an EL_x800 Universal Microplate Reader (Bio-Tek Instruments, Inc.) at 595 nm; the absorbance of untreated cells was designated as 100%, and cell survival expressed as a percentage of this value. The cytotoxicity of oxaliplatin and 17-AAG as single agents or in combination against four colon cancer cell lines HCT116, HT29, DLD1 and SW480 was determined previously [13]. Here we show isobologram analysis as another indicator of the cytotoxicity of the combination: isobolograms were generated as described in [16] according to [17].

2.5. Lactate dehydrogenase (LDH) assay

Cells were plated into 12-well plates (1×10^5 cells per well) and 24 h later, washed with fresh media, and treated with oxaliplatin and 17-AAG for 48 h (time period required for induction of detectable cell death, which was determined experimentally). Apoptotic (floating) and viable (adherent) cells were then separated from the culture medium, the LDH

content of which reflected its release from necrotic cells after breakdown of the plasma membrane. The LDH content of viable or dead cellular subpopulations was further measured using CytoTox96 (Promega) in accordance with the manufacturer's procedure. Briefly, freshly prepared reagent was added to 96-well plates with 50 μl of culture medium, or to cellular samples lyzed in 0.1% NP-40. The amount of LDH was quantified using an EL_x800 Universal Microplate Reader (Bio-Tek Instruments) at an absorbance of 490 nm. Apoptotic or necrotic cell death in treated or control samples were determined as a percentage of LDH detected in the floating cell fraction or in the culture medium, respectively, with total LDH designated as 100%. For viability evaluation the amounts of LDH measured in adherent cellular subpopulations from treated samples were expressed as fractions of the total LDH detected in viable cells from control samples. The expected additive surviving fractions were calculated as the product of actual surviving fractions when treatments were given separately.

2.6. Protein extract preparation and Western blot analysis

Protein extracts were prepared as described previously [18]. Western blotting was carried out according to standard procedures using horseradish peroxidase-conjugated secondary antibodies (Santa Cruz Biotechnology, Santa Cruz, CA) and the ECL + Plus detection system (Amersham, Arlington Heights, IL). Immunoblotting with anti-β-actin antibodies was performed to confirm equal protein loading. The following primary antibodies were used: mouse monoclonal antibodies against p53, p21, and FAS, goat polyclonal antibodies against β-actin from Santa Cruz; mouse monoclonal antibodies against caspases 8, 9 and 3 from Oncogene Research Products (Boston, MA). The rest of the antibodies used were from Cell Signaling Technology (Beverly, MA), including both Cell Cycle/Checkpoint and Regulation Sampler Kits.

2.7. Cell cycle analysis

Cells were plated into 100 mm dishes (1×10^6 cells/dish) and 24 h later starved with serum free medium for 40 h. After starvation fresh media with or without drugs was added for 24 h, followed by the preparation of samples for FACS analysis. Briefly, cells were trypsinized, washed with PBS/0.5% FBS and fixed in 70% ethanol at −20 °C. After subsequent washes cells were resuspended in 1 ml of PBS/0.5% FBS, containing 40 U/ml of RNAse A, stained with propidium iodide (25 μg/ml) for 30 min at 37 °C and analyzed for DNA content. Flow cytometry was performed with FACScan flow cytometer (Becton-Dickinson, San Jose, CA) and CellQuest acquisition/analysis software (Becton-Dickinson). Quantitative analysis of cell cycle distribution was performed using ModFit LT Macintosh software (Verity Software House, Inc., Topsham, ME).

2.8. Terminal dUTP nucleotide end labeling (TUNEL) assay by flow cytometry

Cells were plated into 100 mm dishes (1×10^6 cells/dish), processed as described for cell cycle analysis and treated with drugs for 48 h. The TUNEL assay was performed using APO-DIRECT kit (Pharmingen, BD Biosciences, San Diego, CA) according to the manufacturer's recommendations. Briefly, 1×10^6 cells were fixed with 2% (w/v) electromicroscopic grade paraformaldehyde in PBS on ice for 1 h. After centrifugation, cells were resuspended in ice-cold 70% ethanol and incubated overnight at −20 °C for permeabilization. Cells were washed twice with PBS/0.2% BSA, pelleted and incubated at 37 °C for 2 h with staining solution containing TdT enzyme and 2′-deoxyuridine 5′-triphosphate (FITC-dUTP). After two washes with PBS, the pellet was resuspended in a propidium iodide/RNase A solution, incubated for 60 min in the dark, and analyzed by flow cytometry (see above). Quantitative analysis of apoptosis was performed using FlowJo program (Tree Star, Ashland, OR).

2.9. Colony-forming assays

Colony-forming assays were carried out as previously described [13]. Cells were plated at the density of 300 per well into 6-well plates and after 24 h exposed to oxaliplatin in the presence or absence of cdk2 inhibitor (1 μM) for 72 h. Cells were cultivated in drug-free media for additional 7–10 days. Colonies were stained with Coomassie Blue and counted manually. All experiments were performed at least three times in duplicate.

2.10. Statistical analysis

Data combined from at least three independent experiments were analyzed with unpaired Student's test: $P < 0.05$ was accepted as a statistically significant difference compared with corresponding control. In figure legends: $^{*}P < 0.1$; $^{**}P < 0.05$.

3. Results

3.1. Differential cytostatic but not cytotoxic effects of oxaliplatin and 17-AAG in colon cancer cell lines with different p53 status

In a previous study of the efficacy of the oxaliplatin/17-AAG combination, combination indices (CI) differed according to the assay (MTT, colony-forming) in some of the cell lines [13]. The colony-forming assay predicted synergy or additivity between the treatments, while the MTT assay showed additivity or antagonism (Fig. 1A). The discordance in the results between these two assays suggested an effect of the oxaliplatin/17-AAG combination on cell proliferation, possibly distinct from that on survival. We therefore decided to further explore the events leading to cell death from this combination.

Oxaliplatin has been reported to cause cell death both by apoptosis and necrosis [14]. We used a colorimetric LDH assay to simultaneously quantitate by LDH content the viable (adherent), and apoptotic (floating) cellular sub-populations, while LDH released into the medium after breakdown of the plasma membrane reflected necrotic cell death. In agreement with the results of MTT analysis (Fig. 1A), the LDH-based quantitation of viable (adherent) cells after treatment with low concentrations of both drugs ($1 \times IC_{50}$ for each drug for 72 h)

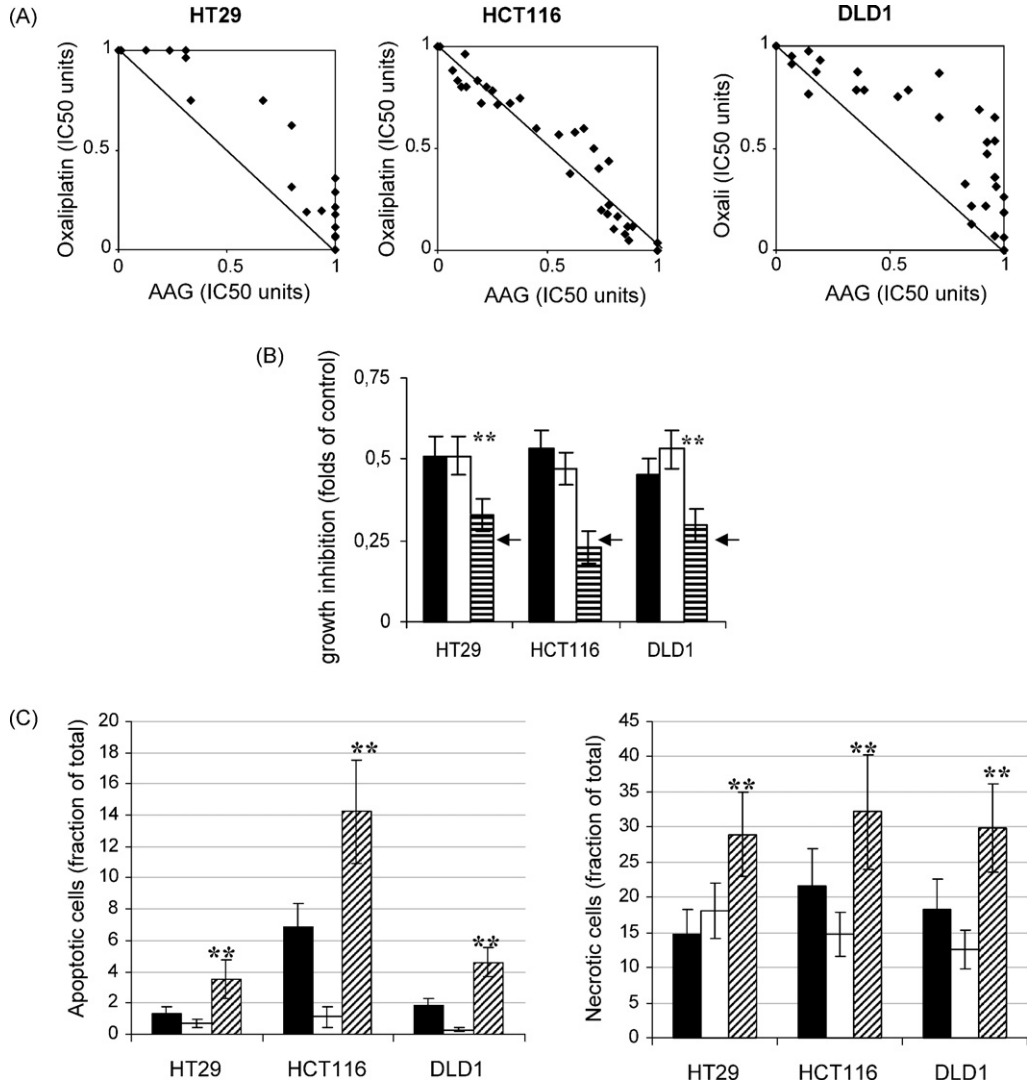

Fig. 1 – Differential cytostatic but not cytotoxic effects of combined oxaliplatin and 17-AAG in colon cancer cell lines with different p53 status. (A) Shown here are the isobolograms at IC_{50} based on the results of MTT assays: cells were treated with a combination of oxaliplatin and 17-AAG for 72 h. Each diagram combines the results of at least three independent experiments in triplicate. (B) Results of LDH assays after treatment for 72 h with oxaliplatin or/and 17-AAG at the concentrations of 1× IC_{50}: graphs demonstrate the decrease of the viable (adherent) cellular fraction in samples treated with individual drugs or with the combination as compared to untreated control. The expected additive surviving fractions were calculated as the product of actual surviving fractions when treatments were given separately and are marked by arrows ($P < 0.05$, actual vs. expected surviving fraction). Black, white and hatched columns represent oxaliplatin, 17-AAG and the combination, respectively. Average values from three independent experiments in duplicate are shown; bars represent standard deviation. (C) Results of LDH assays following drug treatment as described in Section 2: apoptotic (left panel) or necrotic (right panel) cell death in treated samples presented as a percentage of LDH detected in the floating cell fraction or in culture medium, respectively, with total LDH content from dead and alive (adherent) cells designated as 100%. Basal cell death measured in control samples was deducted. Black, white and hatched columns represent oxaliplatin, 17-AAG and the combination, respectively. Average values from three independent experiments in duplicates are shown; bars represent standard deviation (**$P < 0.05$, combination vs. single agents).**

demonstrated additive antiproliferative activity of oxaliplatin/17-AAG in HCT116 cells (Fig. 1B), whereas in HT29 and DLD1 lines the survival fractions were higher than expected from the product of the single agent survival fractions ($P < 0.05$).

We then analyzed apoptotic and necrotic populations after exposure of cells to oxaliplatin and 17-AAG (Fig. 1C). The figure shows the proportions of apoptotic cells (left panel), and those dying by necrosis (right panel) as a percentage of the total number of cells at 48 h after treatment. The apoptotic fractions in adherent cells, as established by TUNEL, were mostly below 0.5% (data not shown). Enhanced cell death from the combination was observed in all three-cell lines ($P < 0.05$).

This assay also revealed that both necrosis and apoptosis are enhanced with the combination, the latter more markedly in the p53-positive HCT116 line. The potential of 17-AAG to enhance cell death from oxaliplatin in colorectal cancer cells is suggested by these findings.

3.2. *Effect of 17-AAG on oxaliplatin-induced changes in cell cycle is due to its ability to inhibit G1 cyclin/cdk complexes*

We next investigated the cell cycle effects of the treatments to better understand the antiproliferative component of the interaction. Cells were synchronized by starvation in serum-free medium (which led up to 70% of cells arrested in G1), treated with oxaliplatin/17-AAG in combination for 24 h, and analyzed for DNA content by FACS. 17-AAG caused inhibition of entry into S-phase in all cell lines irrespective of p53 status (Fig. 2A). Oxaliplatin induced both G1 and G2 arrest in the p53-positive HCT116 cells, but substantially less G1 arrest, and prominent S-phase delay in HT29 and DLD1. With combined treatment, HCT116 cells displayed a similar profile as with 17-AAG and oxaliplatin alone, while HT29 and DLD1 cells demonstrated enhanced G1 arrest with a striking diminution of the oxaliplatin-induced S-phase delay. In effect the combination potentiated the cell cycle effects of the single agents in HCT116, and appeared to neutralize them in the other two cell lines, as shown graphically in Fig. 2B.

To analyze the underlying biochemical mechanisms, we investigated how oxaliplatin- and 17-AAG-induced signaling integrates into both the sequential induction of the cyclin-cdk complexes regulating cell cycle progression, and the activation of checkpoints that result in cell cycle arrest [19]. The regulation of cell cycle progression was analyzed by Western blot analysis of the early and late G1 cyclin/cdk complexes, the cdk inhibitor p21/WAF1, and phosphorylation of Rb (retinoblastoma gene product) (Fig. 3, left panel). In all of the cell lines, oxaliplatin treatment alone resulted in increases in cyclin D1 and cdk4 expression to varying degrees, with no effect on cdk6. The addition of 17-AAG resulted in significant reduction in content of all three proteins, consistent with the known role of Hsp90 in maintaining their stability [20,21]. 17-AAG does not affect the cellular content of Hsp90 itself, but its inhibitory effect on cell lines studied was confirmed by overexpression of

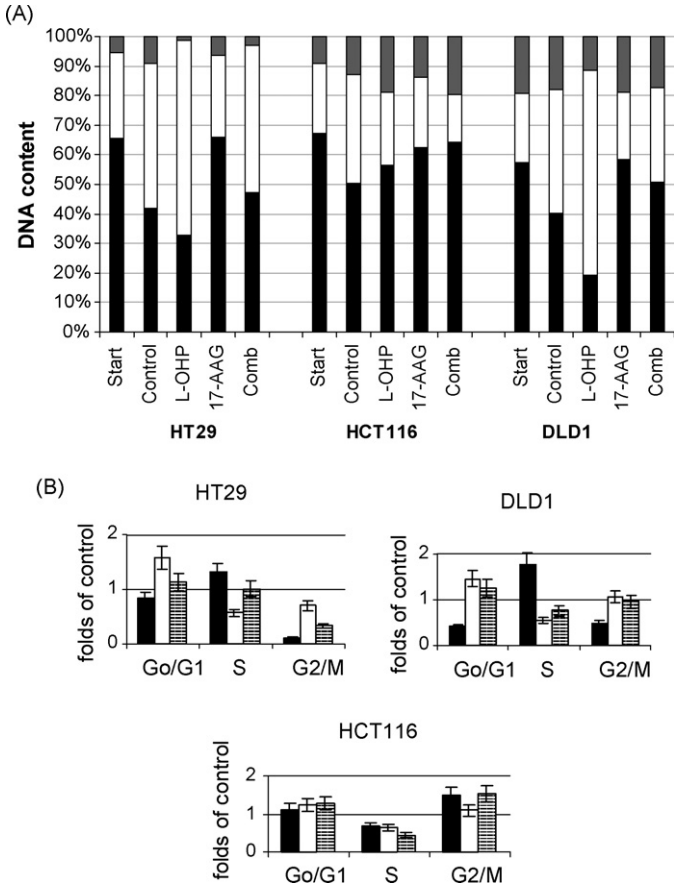

Fig. 2 – 17-AAG modulates cell cycle effects of oxaliplatin in colon cancer cell lines. (A) Cells were starved for 40 h in serum free medium followed by 24 h of drug exposure and cell cycle analysis as described in Section 2. The graph demonstrates the percentage of cells in each phase of cell cycle (total cell count is designated as 100%), with black, white and gray parts of each bar representing G1, S and G2/M phases, respectively. "Start" bars present cell cycle distributions of starved cells. The average results from two independent experiments are presented. (B) Changes in the percentage of cells in G0/G1, S and G2/M after treatment, normalized to the cell cycle distribution of exponentially growing untreated control cells (given the value of 1), are presented. Black, white and hatched columns represent oxaliplatin, 17-AAG and the combination, respectively. Average values from two independent experiments are shown, bars represent standard deviation.

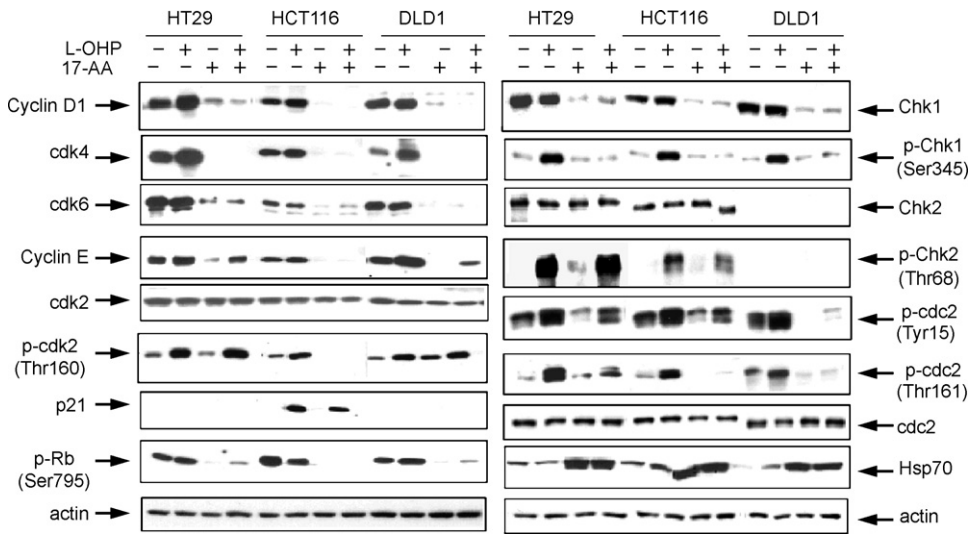

Fig. 3 – Effects of 17-AAG on oxaliplatin-induced expression of cyclin/cdk complexes (left panel) and DNA-damage response proteins (right panel) in colon cancer cells. Cells were treated as described in Fig. 2, followed by protein extracts isolation, electrophoresis and Western blot analysis. Picture shown is representative of three independent experiments.

Hsp70 (Fig. 3, right panel), which is commonly accepted as one of the major characteristics of Hsp90 inhibition by ansamycins [12]. These alterations in cyclin D1, cdk4 and cdk6 did not therefore reflect the cell cycle changes described above.

Changes in cyclin E and in phospho-cdk2 were also observed: increases in response to oxaliplatin and decreases with 17-AAG were seen in all cell lines. With the combination, however, the effects on cyclin E and phospho-cdk2 were substantially greater in HCT116, in which the content of both was reduced to an undetectable level. Cyclin E content was restored in the p53-deficient lines treated with combined therapy (partially in DLD1 cells and to a levels comparable to those in untreated cells in HT29 cell line), suggesting that the addition of 17-AAG served to reverse effects that may have contributed to S-phase delay following oxaliplatin treatment. In these cells also, phospho-cdk2 content was similar to that in oxaliplatin alone treated cells, perhaps implying the cyclin E content was rate-limiting for cell cycle progression under these circumstances. Thus, the addition of oxaliplatin results in elevated expression of the components of G1 cyclin/cdk complexes (most likely through AP-1 mediated transcriptional activation [22]) followed by stabilization of phospho-Rb and G1/S progression in p53-deficient cell lines. In HCT116 cells these effects are opposed by the induction of the cyclin/cdk inhibitor p21/WAF1 [23], and hypophosphorylation of Rb (Fig. 3, left panel). In the p53-negative cell lines, reversal of oxaliplatin-induced stimulation of cyclins and cdk's appears to be a result of the effect of 17-AAG at the level of cdk2-cyclin E, supported by resulting hypophosphorylation of Rb. These data identify cyclins as key targets in the action of 17-AAG in sensitizing cells to oxaliplatin.

The effects of 17-AAG on oxaliplatin-induced checkpoint activation are illustrated in the right panel of Fig. 3. The response of Chk1 (checkpoint kinase 1) to oxaliplatin is consistent with ATM/ATR-dependent (ataxia-telangiectasia, mutated/ATM and Rad3 related) phosphorylation (at Ser345), and destabilization of the protein with 17-AAG [24] in all cell lines. Chk2 phosphorylation (at Thr68) was also induced by oxaliplatin, and was unaffected by 17-AAG in both HT29 and HCT116, while in DLD expression of Chk2 was not detected. Regulation of cdc2 through the both inhibitory (on Tyr15, mediated by Chk1/2 dependent inactivation of cdc25 phosphatase) and activating (on Thr68 by CAK (cdk-activating kinase)) phosphorylation was also observed. Phosphorylation of cdc2 on both residues was induced by oxaliplatin, and then attenuated (both residues in HT29 and Tyr15 in HCT116) or markedly reduced (DLD1, both residues; HCT116, Thr161) by 17-AAG. These results suggest that variable effects of 17-AAG on cdc2 activation status (but not expression level) might determine the differences between cell lines in regards to G2/M block.

3.3. *Activation of apoptotic pathways by oxaliplatin is greater in the p53-positive HCT116 cells, but is facilitated by 17-AAG in all cell lines*

To further quantify the effects of oxaliplatin and 17-AAG alone and in combination on apoptosis, we performed TUNEL analysis with simultaneous monitoring of DNA content to indicate cell cycle distribution at 48 h of treatment (no detectable levels of apoptosis were observed at 24 h). As shown in Fig. 4A, the proportion of apoptotic cells was increased by oxaliplatin only in HCT116, and by 17-AAG in none of the cell lines. When the drugs were used in combination, induction of apoptosis was observed in all cell lines. The absolute proportion of apoptotic cells was highest in HCT116 (to 13.5%), but the degree to which apoptosis was increased was also substantial in HT29 and DLD1 (3% of the cells).

To investigate further the effect of the combination on biochemical events associated with apoptosis, we analyzed markers of caspase activation (Fig. 4B). As expected, apoptotic pathways are activated to a greater extent in HCT116 cells. In the latter, we investigated the effect of these treatments on p53 and FAS, which mediates p53-induced apoptosis through the extrinsic pathway, and found activation by oxaliplatin as predicted [25]. However FAS expression was not further

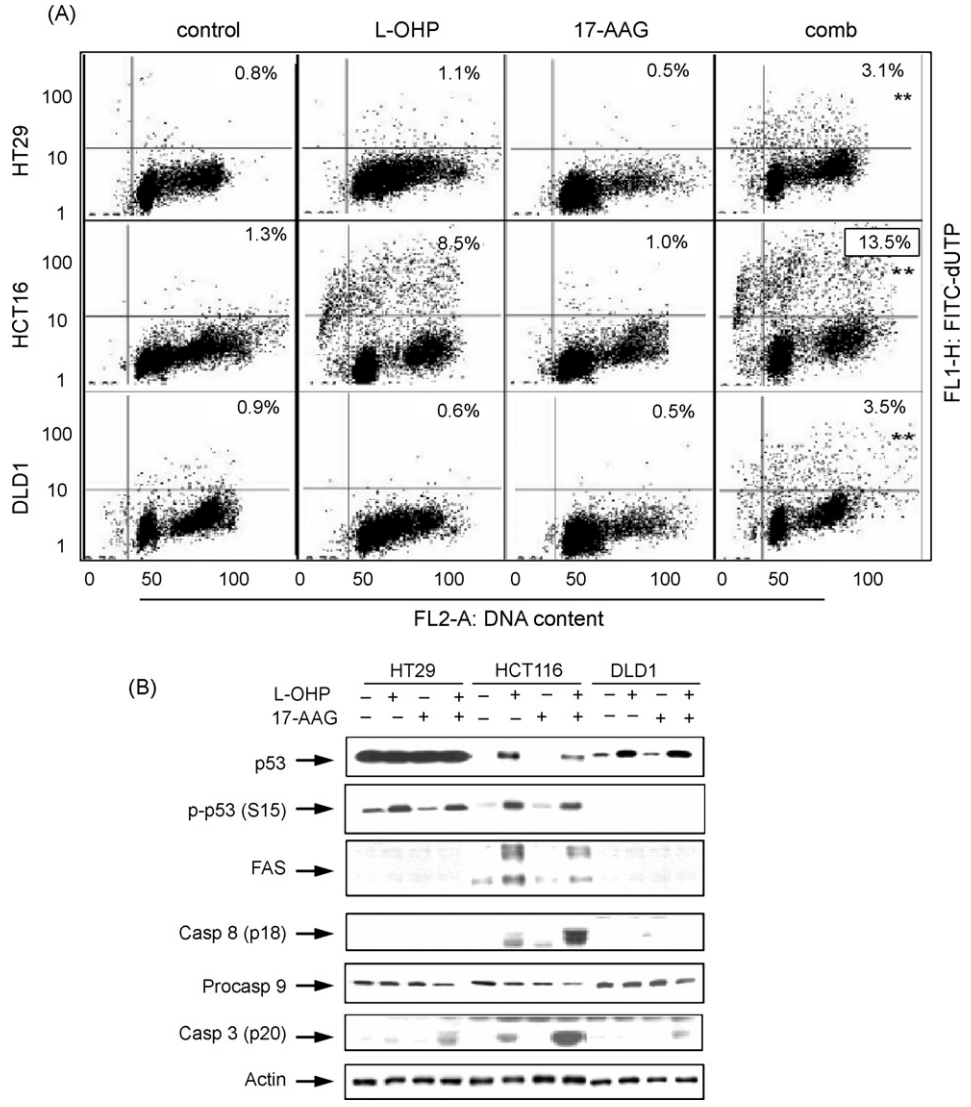

Fig. 4 – Oxaliplatin-induced apoptosis is greater in HCT116 cells, but may be facilitated by 17-AAG in all cell lines. (A) Cells were treated with oxaliplatin or/and 17-AAG for 48 h followed by TUNEL assay as described in Section 2. Picture of the representative experiment is presented. The X-axis shows DNA content determined by propidium iodide staining, and the Y-axis depicts DNA fragmentation determined by FITC-dUTP incorporation. The mean values of apoptotic cells (presented as percentage of total population assessed) are indicated ($P < 0.05$, combination vs. single agents). (B) After drug treatment (as above), protein extracts were isolated and analyzed for activation status of p53, FAS and caspases by Western blotting. The picture shown is representative of three independent experiments.**

increased by the combination; therefore 17-AAG may facilitate oxaliplatin-induced apoptosis downstream of FAS, through inhibition of NF-κB antiapoptotic signaling which we and others have previously shown to be one of the mechanisms involved [13,26]. Activation of caspase 3 by oxaliplatin was increased by the addition of 17-AAG in all cell lines, consistent with the TUNEL findings.

3.4. *Enhancement of oxaliplatin-induced cytotoxicity after introduction of p21 in HCT116 $p53^{-/-}$ cells correlates with abrogation of S-phase delay*

The induction of p21 in HCT16 cells (Fig. 3) supported a positive role for cell cycle inhibition in maximizing oxaliplatin cytotoxicity. To confirm such a role for p21 (as an endogenous cdk inhibitor) in the cytotoxicity of oxaliplatin we used cell lines engineered to have altered function in this pathway: HCT116, HCT116 $p53^{-/-}$, and HCT116 $p53^{-/-}$ expressing p21 (HCTp53-/p21). These cell lines were used for the evaluation of oxaliplatin-induced cell death and cell cycle arrest. Oxaliplatin was added at a concentration of 10 μM (15× IC_{50} for parental HCT116). We used transient transfections, since stable p21 transfectants in a $p53^{-/-}$ background were not viable, consistent with previous results [27]. The expression levels of p53 and p21 were monitored by Western blotting, and expression of the latter was evident for up to 72 h post-transfection. Fig. 5A demonstrates the expected induction of p53 and p21 only in HCT116, and the stable expression of p21

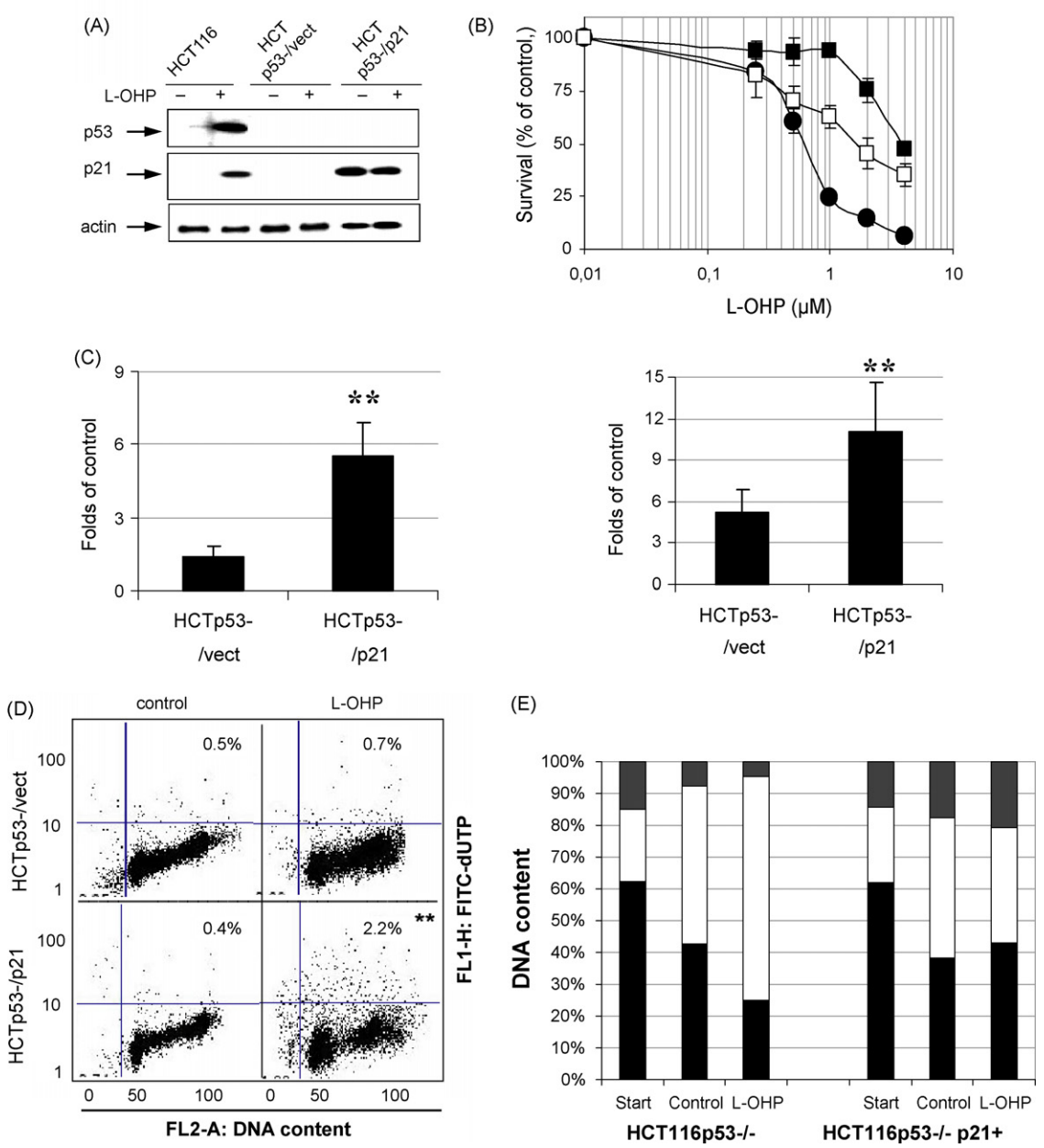

Fig. 5 – S-phase arrest induced by oxaliplatin in p53$^{-/-}$ HCT116 is reversed by introduction of p21/WAF1 with partial restoration of both apoptosis and necrosis. HCT116p53$^{-/-}$ cells transfected with pcDNA3 (HCTp53-/vect) or with pcDNA3-p21 plasmids (HCTp53-/p21) were treated with oxaliplatin and subjected to MTT, LDH assay, TUNEL and cell cycle analysis. Three independent transfection experiments were performed. (A) Typical level of expression of p53 and p21/WAF1 in parental HCT116, HCT p53-/vect and HCTp53-/p21 in the cells collected for cell cycle analysis. (B) 20 h after transfection cells were plated for MTT assays and treated with oxaliplatin for 72 h. Survival curves for HCT116 (closed circle), HCT p53-/vect (closed square) and HCTp53-/p21 (open square) are shown. (C) Results of LDH assays in HCT p53-/vect and HCTp53-/p21 cells treated as described in Fig. 1. Fractions of apoptotic (left panel) or necrotic (right panel) cells (calculated as in Fig. 1B) are presented here in folds increase as compared to untreated control ($P < 0.05$, p21 vs. vector, $n = 3$). (D) Shown is a representative TUNEL experiment; the mean values of apoptotic cells (presented as percentage of total population assessed) are indicated (**$P < 0.05$, p21 vs. vector, $n = 3$). (E), The graph shows the cell cycle distribution after oxaliplatin treatment (as described in legend for Fig. 2A); the average values from three independent experiments are presented.**

in HCT116p53-/p21. Survival curves for HCT116, HCTp53-/vect, and HCT116p53-/p21 cells treated with oxaliplatin are shown (Fig. 5B). Loss of p53 from HCT116 renders the cells resistant to oxaliplatin in vitro (IC_{50} 0.71 μM versus 2.35 μM). Restoration of p21 function restores sensitivity close to that of the parental line (IC_{50} 1.2 μM). Similar effects on apoptotic and necrotic cell death, as determined by LDH or TUNEL assays, were observed (Fig. 5C and D). Loss of p53 abrogated the apoptotic response to

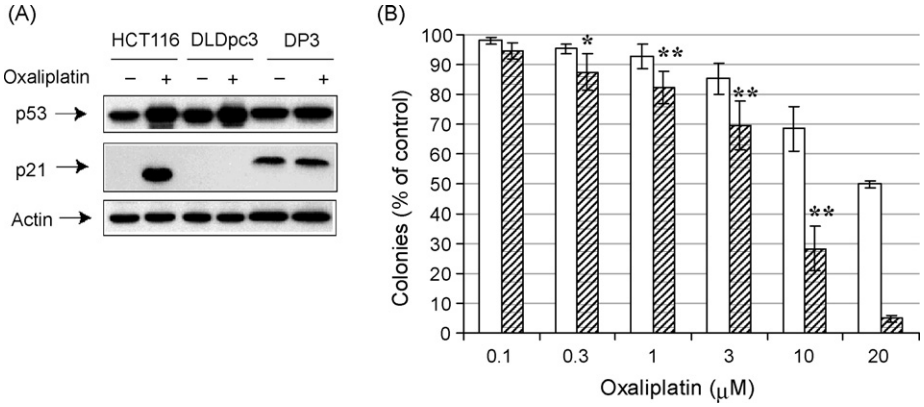

Fig. 6 – Introduction of p21 into DLD1 cell line results in enhancement of oxaliplatin cytotoxicity in colony-forming assays. (A) Shown is western analysis of p21 expression in DLDpc3, DP3 and HCT116 cells treated with 30 μM oxaliplatin for 24 h. (B) Results of colony-forming assays presented as surviving colonies (percentage of untreated control). Open and hatched columns represent DLDpc3 and DP3, respectively; shown are the average values of at least three independent experiments in duplicate, bars represent standard deviation, *P < 0.1, **P < 0.05 (p21 vs. empty vector).

oxaliplatin completely (0.7% versus 8.5% in the parental line [Fig. 2]), while restoration of p21 partially rescued the capacity to enter apoptosis (2.2% versus 0.7%) (Fig. 5D). A cell cycle analysis also revealed that p21-dependent facilitation of apoptosis correlated with changes in cell cycle distribution, similar to those induced by 17-AAG in p53-deficient cells treated with oxaliplatin (Fig. 5E). The HCT116p53$^{-/-}$ cells showed a profile of S-phase delay similar to HT29 and DLD1, supporting the contribution of the p53 loss in these cell lines, and not some other abnormality, in determining the cell cycle profile that differed from HCT116. The effect of restoring p21 was to abrogate the S-phase delay, thus implicating inactivation of the p21 pathway in its causation.

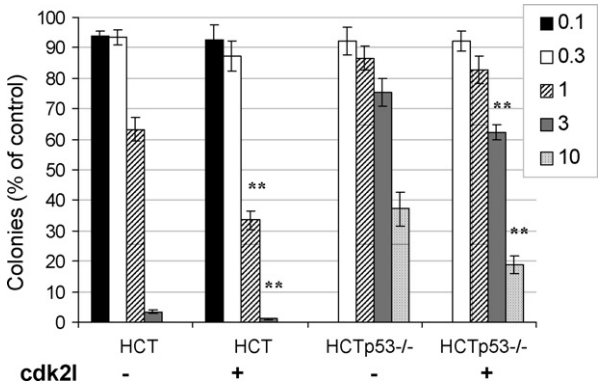

Fig. 7 – Inhibition of cdk2 potentiates oxaliplatin-induced cell death in colon cancer cells. HCT116 and HCT116p53$^{-/-}$ cells were treated with 1 μM of cdk2I for 1 h prior to addition of oxaliplatin followed by colony-forming assays. Cells were treated with various concentrations of oxaliplatin for 72 h. Results are presented as the number of surviving colonies (percentage of untreated control); concentration of oxaliplatin is shown in box to the right. Graph shows the average values of three independent experiments in duplicate; bars represent standard deviation, **P < 0.05 (cdk2I vs. control).

To confirm that the effect of p21 (as a cell cycle modulator) on oxaliplatin cytotoxicity in HCT116p53$^{-/-}$ was not cell line specific, we expressed p21 in another p53-deficient cell line, DLD1. The efficiency of the transfection of these cells was significantly lower than in HCT116p53$^{-/-}$, but we were able to isolate a DLD1-derived cell line (DP3), stably expressing p21 (Fig. 6A). A colony-forming assay, which was the most reliable analysis for quantification of the cell death, performed on the DP3 and control cell line DLDpc3 (expressing empty vector), revealed the decrease in the survival of p21-proficient cells (Fig. 6B), with a three-fold decrease in IC_{50} for oxaliplatin.

3.5. *Inhibition of cdk2 is associated with enhanced oxaliplatin cytotoxicity*

Since the differential cell cycle response to the oxaliplatin/17-AAG combination was associated with changes at the level of cyclinE/cdk2 (Fig. 4A), we inhibited G1/S transition by a specific cdk2 inhibitor, cdk2I, and determined cell death after oxaliplatin treatment. Initial MTT assays revealed differential responses of cell lines to cdk2I: HT29 were the most resistant to growth inhibition ($IC_{50} > 5$ μM), whereas a concentration of 2.5 μM was sufficient to cause 50% growth inhibition in HCT116, HCT116p53$^{-/-}$ and DLD1 cell lines (data not shown). Results of colony-forming assays (Fig. 7) demonstrated enhancement of oxaliplatin cytotoxicity in HCT116 and HCT116p53$^{-/-}$ cell lines in the presence of cdk2 inhibition (1 μM of cdk2I was added 1 h prior to oxaliplatin and did not affect colony counts in controls), with HCT116 cells being more sensitive than its p53-deficient derivative: IC_{50} values were decreased 2-fold in HCT116 versus 1.7-fold in HCT116p53$^{-/-}$, $P < 0.05$ for both. The decrease in IC_{50} for oxaliplatin in the presence of cdk2I was 1.5-fold in DLD1 cell line ($P < 0.05$) [data not shown].

4. Discussion

The effectiveness of cytotoxic drugs on malignant cells is often associated with their capacity to inhibit cellular proliferation

and to induce apoptosis, or programmed cell death. But the view that apoptosis represents the major mechanism by which tumor cells are killed may not be applicable to all cytotoxics. Cells with reduced apoptotic capabilities that have suffered excessive DNA damage die by necrosis, representing passive, lytic cell death mediated by ATP depletion [28]. Key elements of the cell death pathways, including apoptosis as one possible outcome, overlap with other complex signaling systems, such as cell cycle control, DNA damage response, or stress signaling, and investigation of these fundamental cellular mechanisms in cells treated with cytotoxic drugs may have broad clinical relevance. In this study we have shown the activation of both apoptosis and necrosis by the combination of oxaliplatin and 17-AAG. We also show that the MTT assay fails to quantitate accurately the cell death levels that are a consequence of the interaction of oxaliplatin and 17-AAG in colon cancer cell lines. We found the basis of this to lie in the cell cycle effects of both oxaliplatin and 17-AAG. We found further that reversal of S-phase delay, caused by lack of p53 function in HT29 and DLD1 cells and abrogated by 17-AAG's cell cycle effects, results in greater cell death. These findings implicate cell cycle abnormalities consequent upon p53 mutation as key components in cytotoxic responses to oxaliplatin.

In our previous work we studied the interaction of Hsp90 inhibitors with cisplatin in colon cancer cell lines [16] and showed the importance of a p53-dependent FAS-mediated apoptotic cascade in cytotoxicity of cisplatin alone or in combination with geldanamycin and 17-AAG [29]. We have also shown that down-regulation of pro-survival signaling through the transcription factor NF-κB contributes to the positive interaction between 17-AAG and oxaliplatin [13]. In these studies we measured apoptosis as the main indicator of cellular response to the therapy, but a role for growth inhibition and non-apoptotic cell death must also be considered [7,30]. The aim of the current study was to characterize the balance between antiproliferative effects and cell death (by necrosis and apoptosis) induced by oxaliplatin alone, and in combination with 17-AAG.

When 17-AAG and other benzoquinone ansamycins are used as single agents they display cell-specific cytotoxic effects. We have been unable to detect the activation of caspases and robust induction of apoptosis by 17-AAG or geldanamycin in colon cancer cell lines [13,16,29], though in other models such activation is observed inconsistently [31–33]. Participation of both extrinsic and intrinsic apoptotic pathways in response to oxaliplatin was observed in the p53-positive HCT116 cells, characterized by the induction of Fas receptor and caspase 8 cleavage, as well as by processing of caspase 9, and apoptosis was increased by 17-AAG (Fig. 4B). In the p53-deficient cell lines, while induction of the extrinsic apoptotic pathway could not be detected, enhancement of mitochondrial apoptosis was observed with combined oxaliplatin and 17-AAG (Fig. 4B). Various mechanisms underlying the positive interactions of Hsp90 inhibitors and genotoxic drugs have been proposed, including the down-regulation of pro-survival signaling through NF-κB [26,13] and AKT [34], and cell cycle interference through disruption of G1 cyclin/cdk complexes [21] or Chk1 [24] among others. There have been no reports of necrotic cell death caused by 17-AAG alone, but in this study, LDH assays showed the additivity of necrotic responses induced by each drug alone in all cell lines treated with the oxaliplatin/17-AAG combination. It should be noted, however, that the LDH most likely measures the accumulated total of necrotic cells, while the apoptotic fraction represents an instantaneous quantitation, so direct comparison of the percentages of necrotic and apoptotic cells in the same treatment may not be appropriate. It is of value however for analysis of the relative effects of various treatments in different cell lines, in parallel with other methods of cell death evaluation. The impact of the addition of 17-AAG to oxaliplatin on both apoptosis and necrosis in these cell lines appears to relate to the cell cycle effects of the combination, suggesting avenues for therapeutic development.

The role of p53 as a possible determinant of oxaliplatin resistance is controversial [9]. p53 regulates apoptosis, DNA repair and cell cycle arrest, and is mutated or otherwise inactivated in over 50% of cases of colorectal cancer [35]. The cytotoxic effects of oxaliplatin have been evaluated in colon cancer cell lines with differing genetic backgrounds [11,36] and in isogenic derivatives of HCT116 cells in which p53 function has been modified [5,8,10]. The conclusions of these studies have been contradictory, assigning a role for p53 in oxaliplatin-induced cytotoxicity from important [5,10] to marginal [8,36]. Proposed mechanisms of oxaliplatin-induced cell death include both p53- and Bax-dependent [10] and p53-independent apoptosis, with the latter mediated either by Fas [11] or by the Bcl2 family proteins Bax and Bak [8]. A study that analyzed both the isogenic HCT116 system, as well as a panel of colorectal cancer cell lines, emphasized the paradoxical role of p53: despite its clear role in the apoptotic response to oxaliplatin in HCT116 cells, p53 expression had limited predictive value for 30 independent cell lines [9]. These findings are consistent with previous analyses of tumor p53 in series of patients treated uniformly [37], in that an independent role for p53 as a marker of either survival or of outcome from therapy cannot be demonstrated. The data presented here demonstrate that p53 cannot be the sole determinant of oxaliplatin cytotoxicity, but that its cell cycle effects may positively modulate the efficacy of oxaliplatin.

Oxaliplatin-induced p53-dependent G1 arrest mediated through p21 has been reported for HCT116 and its derivative cell lines [10], while in HT29 cells an S-phase block was demonstrated [14]. Additive antiproliferative effects of the oxaliplatin/17-AAG combination, which we demonstrate here, also required functional p53. The enhancement of cell cycle arrest in HCT116 cells in the presence of 17-AAG could result from either direct inhibition of Hsp90, leading to destabilization of the existing cyclin/cdk complexes [21], or an indirect negative effect on the induction of cyclins and cdks through inhibition of oxaliplatin-induced transcriptional activation of AP-1 and NF-κB [13]. Therefore, in p53-proficient cells p21 was a key determinant of cooperation between oxaliplatin and 17-AAG in inhibiting proliferation. In p53-deficient cell lines 17-AAG compromised oxaliplatin-induced S-phase delay by partially inhibiting G1/S progression, through an effect as noted above, principally on late G1 kinases. We hypothesized that the 17-AAG-enhanced G1 arrest acts to mimic the effects of p21 in p53-negative cells. This proposition was confirmed in experiments involving reintroduction of p21 into a p53-deficient derivative of HCT116 cell line. Hayward et al. [10]

demonstrated higher sensitivity of HCT116 $p21^{-/-}$ cells to oxaliplatin, which implies the protective role for p21. However, the cells used in this study were p53-proficient, and while the ability of p53 to cause cell cycle arrest was diminished (through knock down of p21 gene), its apoptotic functions were not affected. We believe, therefore, that this cellular model does not fully reflect the effect of p21 in a p53-negative background, and hence our data are not in conflict with Hayward et al. [10]. When we used the approach described above, the introduction of p21 into HCT116 $p53^{-/-}$ and DLD1 cell lines with abrogated p53-dependent apoptotic potential, there was an increase in sensitivity to oxaliplatin. Moreover, the specific inhibition of cdk2 also enhanced oxaliplatin-induced cell death. Consistent with our findings, the deregulation of oxaliplatin-induced G1 arrest has been shown to decrease oxaliplatin efficacy in DLD1 cells [38]. These data suggest that strategies to block signaling pathways leading to S-phase delay induced by oxaliplatin in p53-deficient cells might enhance the apoptotic (and necrotic) response and facilitate oxaliplatin cytotoxicity.

Our conclusions are in accord with the report of a positive correlation of G1 arrest with the cytotoxicity of platinum compounds, including oxaliplatin [39]. The ability of 17-AAG and other Chk1 inhibitors to enhance the cytotoxicity of DNA damaging drugs in p53-deficient cellular models by overcoming S-phase arrest has also been shown [24,40]. Small-molecule cyclin-dependent kinase modulators are being actively studied in preclinical models and clinical trials as single agents and in combination with standard chemotherapy (reviewed in [41]). The abrogation of oxaliplatin-induced S-phase accumulation by 17-AAG or cdk inhibitors, which results in greater oxaliplatin-induced cell death, suggests that cdk modulators may have the potential to enhance oxaliplatin cytotoxicity in colon tumors.

Acknowledgments

This work was supported in part by NIH grant CA 49820.

We thank Dr. Edward Sausville (NCI, Bethesda) for providing 17-AAG, Dr. Bert Vogelstein (John Hopkins Oncology Center, Baltimore, MD) for kindly providing HCT116 $p53^{-/-}$ cells, Dr. M. Olson (University of Pennsylvania, Philadelphia) for the gift of pcDNA3 plasmid expressing p21, and Dr. David Roberts for pcDNA3-eGFP plasmid.

REFERENCES

[1] Johnson SW, Stevenson PJ, O'Dwyer PJ. Cisplatin and its analogues. In: DeVita VT, Hellman S, Rosenberg SA, editors. Cancer: principles and practice of oncology. 6th ed., Philadelphia, USA: Lippincott Williams & Wilkins; 2001. p. 377–88.

[2] Andre T, Boni C, Mounedji-Boudiaf L, Navarro M, Tabernero J, Hickish T, et al. Oxaliplatin, fluorouracil, and leucovorin as adjuvant treatment for colon cancer. N Engl J Med 2004;350:2343–51.

[3] el-Akawi Z, Abu-hadid M, Perez R, Glavy J, Zdanowicz J, Creaven PJ, et al. Altered glutathione metabolism in oxaliplatin resistant ovarian carcinoma cells. Cancer Lett 1996;105:5–14.

[4] Mishima M, Samimi G, Kondo A, Lin X, Howell SB. The cellular pharmacology of oxaliplatin resistance. Eur J Cancer 2002;38:1405–12.

[5] Boyer J, McLean EG, Aroori S, Wilson P, McCulla A, Carey PD, et al. Characterization of p53 wild-type and null isogenic colorectal cancer cell lines resistant to 5-fluorouracil, oxaliplatin, and irinotecan. Clin Cancer Res 2004;10:2158–67.

[6] Hector S, Bolanowska-Higdon W, Zdanowicz J, Hitt S, Pendyala L. In vitro studies on the mechanisms of oxaliplatin resistance. Cancer Chemother Pharmacol 2001;48:398–406.

[7] Arnould S, Hennebelle I, Canal P, Bugat R, Guichard S. Cellular determinants of oxaliplatin sensitivity in colon cancer cell lines. Eur J Cancer 2003;39:112–9.

[8] Gourdier I, Crabbe L, Andreau K, Pau B, Kroemer G. Oxaliplatin-induced mitochondrial apoptotic response of colon carcinoma cells does not require nuclear DNA. Oncogene 2004;23:7449–57.

[9] Arango D, Wilson AJ, Shi Q, Corner GA, Aranes MJ, Nicholas C, et al. Molecular mechanisms of action and prediction of response to oxaliplatin in colorectal cancer cells. Br J Cancer 2004;91:1931–46.

[10] Hayward RL, Macpherson JS, Cummings J, Monia BP, Smyth JF, Jodrell DI. Enhanced oxaliplatin-induced apoptosis following antisense Bcl-xl down-regulation is p53 and Bax dependent: genetic evidence for specificity of the antisense effect. Mol Cancer Ther 2004;3:169–78.

[11] Marchetti P, Galla DA, Russo FP, Ricevuto E, Flati V, Porzio G, et al. Apoptosis induced by oxaliplatin in human colon cancer HCT15 cell line. Anticancer Res 2004;24:219–26.

[12] Neckers L. Heat shock protein 90 inhibition by 17-allylamino-17-demethoxygeldanamycin: a novel therapeutic approach for treating hormone-refractory prostate cancer. Clin Cancer Res 2002;8:962–6.

[13] Rakitina T, Vasilevskaya I, O'Dwyer P. Additive interaction of oxaliplatin and 17-allylamino-17-demethoxygeldanamycin in colon cancer cell lines results from inhibition of nuclear factor kappaB signaling. Cancer Res 2003;63:8600–5.

[14] Arnould S, Guichard S, Hennebelle I, Cassar G, Bugat R, Canal P. Contribution of apoptosis in the cytotoxicity of the oxaliplatin-irinotecan combination in the HT29 human colon adenocarcinoma cell line. Biochem Pharmacol 2002;64:1215–26.

[15] Coleman ML, Marshall CJ, Olson MF. Ras promotes p21 (Waf1/Cip1) protein stability via a cyclin D1-imposed block in proteasome-mediated degradation. EMBO J 2003;22:2036–46.

[16] Vasilevskaya IA, Rakitina TV, O'Dwyer PJ. Geldanamycin and its 17-allylamino-17-demethoxy analogue (17-AAG) antagonize the action of cisplatin in human colon adenocarcinoma cells: differential caspase activation as a basis for interaction. Cancer Res 2003;63:3241–6.

[17] Tsai CM, Gazdar AF, Venzon DJ, Steinberg SM, Dedrick RL, Mulshine JL, et al. Lack of in Vitro synergy between etoposide and *cis*-diamminedichloroplatinum (II). Cancer Res 1989;49:2390–7.

[18] Vasilevskaya IA, O'Dwyer PJ. Effects of geldanamycin on signaling through activator-protein 1 in hypoxic HT29 human colon adenocarcinoma cells. Cancer Res 1999;59:3935–40.

[19] Shapiro GI, Harper JW. Anticancer drug targets: cell cycle and checkpoint control. J Clin Invest 1999;104:1645–53.

[20] Srethapakdi M, Liu F, Tavorath R, Rosen N. Inhibition of Hsp90 function by ansamycins causes retinoblastoma gene product-dependent G1 arrest. Cancer Res 2000;60:3940–6.

[21] Munster PN, Basso A, Solit D, Norton L, Rosen N. Modulation of Hsp90 function by ansamycins sensitizes breast cancer cells to chemotherapy-induced apoptosis in an RB- and schedule-dependent manner. Clin Cancer Res 2001;7:2228–36.
[22] Shaulian E, Karin M. AP-1 in cell proliferation and survival. Oncogene 2001;20:2390–400.
[23] el-Deiry WS, Tokino T, Velculescu VE, Levy DB, Parsons R, Trent JM, et al. WAF1, a potential mediator of p53 tumor suppression. Cell 1993;75:817–25.
[24] Arlander SJ, Eapen AK, Vroman BT, McDonald RJ, Toft DO, Karnitz LM. Hsp90 inhibition depletes Chk1 and sensitizes tumor cells to replication stress. J Biol Chem 2003;278:52572–7.
[25] HTPetak I, Tillman DM, Harwood FG, Mihalik R, Houghton JA. Fas-dependent and -independent mechanisms of cell death following DNA damage in human colon carcinoma cells. Cancer Res 2000;60:2643–50.
[26] Lewis J, Devin A, Miller A. Disruption of hsp90 function results in degradation of the death domain kinase, receptor-interacting protein (RIP), and blockage of tumor necrosis factor-induced nuclear factor-kappaB activation. J Biol Chem 2000;275: 10519–26.
[27] Kralj M, Husnjak K, Korbler T, Pavelic J. Endogenous p21WAF1/CIP1 status predicts the response of human tumor cells to wild-type p53 and p21WAF1/CIP1 overexpression. Cancer Gene Ther 2003; 10:457–67.
[28] Eguchi Y, Shimizu S, Tsujimoto Y. Intracellular ATP levels determine cell death fate by apoptosis or necrosis. Cancer Res 1997;57:1835–40.
[29] Vasilevskaya IA, Rakitina TV, O'Dwyer PJ. Quantitative effects on c-Jun N-terminal protein kinase signaling determine synergistic interaction of cisplatin and 17-allylamino-17-demethoxygeldanamycin in colon cancer cell lines. Mol Pharmacol 2004;65:235–43.
[30] Faivre S, Chan D, Salinas R, Woynarowska B, Woynarowski JM. DNA strand breaks and apoptosis induced by oxaliplatin in cancer cells. Biochem Pharmacol 2002;66: 225–37.
[31] Park JW, Yeh MW, Wong MG, Lobo M, Hyun WC, Duh QY, et al. The heat-shock protein 90-binding geldanamycin inhibits cancer cell proliferation, down-regulates oncoproteins, and inhibits epidermal growth factor-induced invasion in thyroid cancer cell lines. J Clin Endocrinol Metab 2003;88:3346–53.
[32] Braga-Basaria M, Hardy E, Gottfried R, Burman KD, Saji M, Ringel MD. 17-Allylamino-17-demethoxygeldanamycin activity against thyroid cancer cell lines correlates with heat shock protein 90 levels. J Clin Endocrinol Metab 2004;89:2982–8.
[33] Nimmanapalli R, O'Bryan E, Kuhn D, Yamaguchi H, Wang H-G, Bhalla KN. Regulation of 17-AAG-induced apoptosis: role of Bcl-2, Bcl-xL, and Bax downstream of 17-AAG-mediated down-regulation of AKT. Raf-1 and Src kinases. Neoplasia 2003;102:269–75.
[34] Münster PN, Marchion DC, Basso A, Rosen N. Degradation of HER2 by ansamycins induces growth arrest and apoptosis in cells with HER2 overexpression via a HER3, phosphatidylinositol 3′-kinase-AKT-dependent pathway. Cancer Res 2002;62:3132–7.
[35] Vogelstein B, Lane D, Levine AJ. Surfing the p53 network. Nature 2000;408:307–10.
[36] Sergent C, Franco N, Chapusot C, Lizard-Nacol S, Isambert N, Correia M, et al. Human colon cancer cells surviving high doses of cisplatin or oxaliplatin in vitro are not defective in DNA mismatch repair proteins. Cancer Chemother Pharmacol 2002;49:445–52.
[37] Glasgow SC, Yu J, Carvalho LP, Shannon WD, Fleshman JW, McLeod HL. Unfavourable expression of pharmacologic markers in mucinous colorectal cancer. Br J Cancer 2005;92:259–64.
[38] Hata T, Yamamoto H, Ngan CY, Koi M, Takagi A, Damdisuren B, et al. Role of p21waf1/cip1 in effects of oxaliplatin in colorectal cancer cells. Mol Cancer Ther 2005;4:1585–94.
[39] Vekris A, Meynard D, Haaz MC, Bayssas M, Bonnet J, Robert J. Molecular determinants of the cytotoxicity of platinum compounds: the contribution of in silico research. Cancer Res 2004;64:356–62.
[40] Eastman A, Kohn EA, Brown MK, Rathman J, Livingstone M, Blank DH, et al. A novel indolocarbazole, ICP-1, abrogates DNA damage-induced cell cycle arrest and enhances cytotoxicity: similarities and differences to the cell cycle checkpoint abrogator UCN-01. Mol Cancer Ther 2002;1:1067–78.
[41] Senderowicz AM. Novel small molecule cyclin-dependent kinases modulators in human clinical trials. Cancer Biol Ther 2003;2:S84–95.